

Short Communication

Effect of Co Doping on Structural and Magnetic Properties of ZnO Nanoparticles Synthesized by Novel Combustion Synthesis

V. Rajendar*, K. Venkateswara Rao, K. Shobhan, C.H. Shilpa Chakra

Centre for Nano Science and Technology, Institute of Science and Technology
Jawaharlal Nehru Technological University Hyderabad, India.

(Received 29 December 2012; published online 28 March 2013)

ZnO is a wide band gap semiconductor (3.37 eV) with a high exciton binding energy (60 meV), which has wide applications in advanced optoelectronic devices. The theoretical prediction of room temperature ferromagnetism will be possible through the investigation of diluted magnetic semiconductors such as transition metal doped ZnO, especially Cobalt doped ZnO. The aim of the work is to synthesize $Zn_{1-x}Co_xO$ ($x = 0$ and $x = 0.20$) nanostructures through a novel urea based auto combustion method and its characterization. The Structural and Magnetic studies of the synthesized $Zn_{1-x}Co_xO$ Nano powders were carried out by X-Ray diffraction (XRD) technique and Vibrating Sample Magnetometer (VSM), respectively.

Keywords: Structural, Magnetic properties, Co-doped ZnO, Diluted magnetic semiconductors.

PACS numbers: 81.07.Wx, 81.07.Bc, 81.07. – b, 61.05.cp, 75.50.Pp, 64.70.N

1. INTRODUCTION

Diluted magnetic semiconductors (DMSs) have attracted a great deal of attention due to the exciting features for spintronic studies and possible application (1-3). A fraction of the cations are replaced by magnetic ions in DMS materials because of that complex and interesting electrical and magnetic properties will be exhibited, which are tunable (4). At the beginning of the development in this field, the DMSs based on III-V or II-VI were intensively studied, even though these materials show ferromagnetism only at very low temperatures. The present work focuses on synthesizing Co-doped ZnO powder by a novel urea-based auto combustion method. ZnO doped with small amount of Co^{2+} (i.e. $Zn_{0.8}Co_{0.2}O$) without any modification in the structure has been of the most considerable interest. Therefore the Structural and morphological analysis of the synthesized $Zn_{1-x}Co_xO$ was carried out by X-Ray diffraction (XRD) technique and Vibrating Sample Magnetometer (VSM) (5-8).

2. EXPERIMENTAL PROCEDURE

Preparation: The $Zn_{1-x}Co_xO$ (i.e. $x = 0.0$, $x = 0.20$) Nano powders have been synthesized through a novel auto combustion method using fuel to oxidizer equal to one ($\psi = 1$). Zinc nitrate hexahydrate $Zn(NO_3)_2 \cdot 6H_2O$, cobalt nitrate hexahydrate $Co(NO_3)_2 \cdot 6H_2O$ were used as starting chemicals and urea $Co(NH_2)_2$ as a fuel. These entire chemicals were weighed in stoichiometric proportions and dissolved in 100 ml of distilled water. Then polyethylene glycol was added under constant stirring. After 30 min, the solution completely converted to a highly viscous gel. Next, the beaker vessel was transferred into heat oven to complete the combustion reaction after about 5 min to give fine powders. Two samples, one un-doped and other cobalt doped have been prepared.

The obtained powders were characterized by XRD using Bruker D8 X-ray diffract meter (CuK_{α} $\lambda = 1.5418 \text{ \AA}$) in the range $25^\circ-80^\circ (2\theta)$. Size and magnetic property of the samples were observed by (Lakeshore, Model no: 7410) Vibrating Sample Magnetometer.

3. RESULTS AND DISCUSSION

X-Ray diffraction: The XRD pattern of the obtained samples reveals the formation of cobalt doped zinc oxide. The average crystallite size was measured using the Debye-Scherrer's formula,

$$D = \frac{k\lambda}{\beta \cos \theta}$$

Where, D is the average size of the crystal, λ is the wavelength of X-ray used and K is constant ($K = 1$), β is the full width at the half maximum (FWHM) of the diffraction peak, θ is the Bragg's angle and average

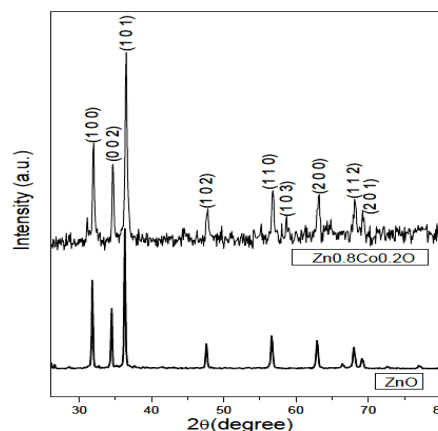


Fig. 1 – XRD patterns of calcined pure ZnO and $Zn_{0.8}Co_{0.2}O$

* vanga.rajendar@gmail.com

sizes were obtained to be 28 nm and 26 nm for the powders of ZnO and Co doped ZnO respectively

The XRD patterns of the calcined ZnO and Co doped ZnO powders matched standard data (JCPDS, 36-1451) as shown in Fig. 1. Only the diffraction lines of the wurtzite ZnO were observed without any other peaks, indicating that the Co has entered ZnO lattice without changing the wurtzite structure.

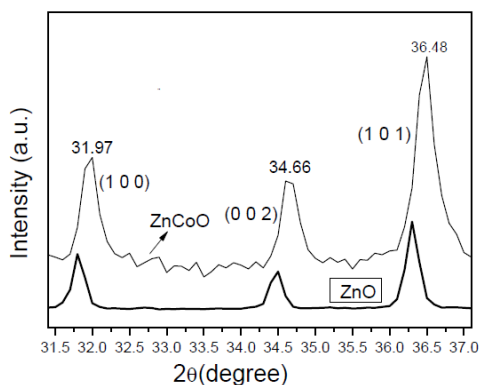


Fig. 2 – Comparison of $Zn_{0.80}Co_{0.20}O$ (100), (002) and (101) peak positions with pure ZnO

ZnO structure lattice parameters compared with the $Zn_{0.80}Co_{0.20}O$, then the unit cell parameters a (3.2324 Å) and c (5.9766 Å) of $Zn_{0.80}Co_{0.20}O$ were smaller than the lattice parameters of ZnO a (3.2485 Å) and c (6.0085 Å). These changes were consistent with the shift of (100), (002) and (101) peaks of $Zn_{0.80}Co_{0.20}O$ powder as shown in Fig. 2.

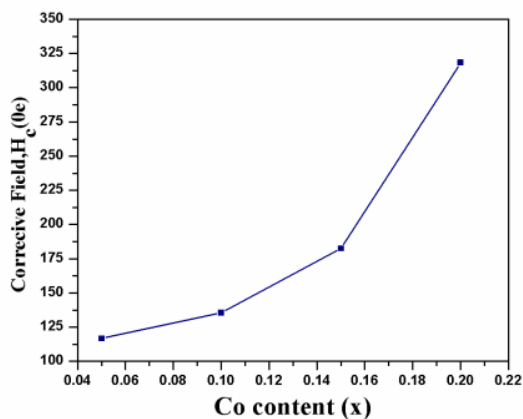


Fig. 3 – Variation of coercive field (H_c) values as the function of Co doping content in $Zn_{1-x}Co_xO$ nanoparticles

We observe that the undoped ZnO sample shows diamagnetic behavior. Co-doped ZnO nanopowders show ferromagnetic behavior at room temperature. From the hysteresis loop, the coercive field (H_c) values are found to increase with increase in Co doping concentrations as shown in Fig. 3. The maximum saturation magnetization was observed for 0.2% Co-doped ZnO nanopowders.

In the present studies, however, no detectable Co or CoO phases could be observed in the XRD spectra. Further, the increase of intensities of Co-related absorption bands in optical spectra and decrease of lattice constant values with increase in Co concentrations suggests sys-

tematic substitution of Co ions in the ZnO lattice. These observations rule out the possibility of ferromagnetism due to unwanted Co precipitates in the samples. In the absence of any unwanted precipitates, the observation of ferromagnetism requires exchange interaction between free delocalized carriers and localized d-spins of Co ions and therefore the presence of free carriers in the samples is a necessary condition for the observations of ferromagnetism. The required free charge carriers might be made available by the presence of multi valence Co ions viz. Co^{2+} and Co^{3+} as well as Valance centers. Further, increase of doping concentrations results in the annihilation of Vicente's, thereby is reducing the overall free charge carrier density. As a result, the dominant magnetic interaction between Co ions becomes nearest neighbour anti-ferromagnetic and ferromagnetic properties gradually decrease after 1 at % Co doping concentration. Hence, to achieve the best ferromagnetic character in these materials, the Concentration of Co dopant has to be properly optimized.

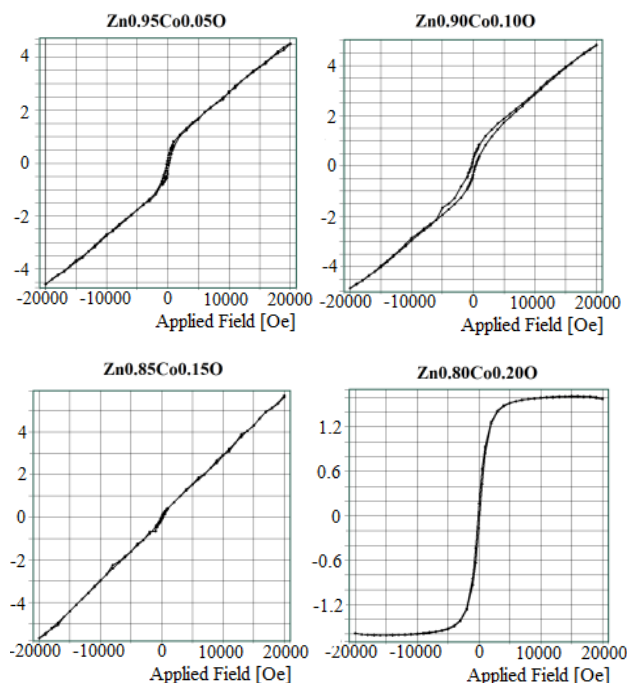


Fig. 4– M-H loop showing hysteresis of Co-doped ZnO. At room temperature magnetization (M) versus applied field (H) study was performed to observe how the concentration of Fe atoms changes the magnetic behavior for $Zn_{1-x}Co_xO$ ($x = 0.05$ to 0.2) nanoparticles using VSM in the field range of 0-21000 T

At room temperature coercive field (H_c) and the remnant magnetization (emu/g) are observed with the increase in the doping concentration correspondingly. The coercive field (H_c) decreases and the remnant magnetization (emu/g) increases with the increase in the concentration, respectively. The decrease and increase in coercive field (H_c) and the remnant magnetization (emu/g) can be observed respectively from the Fig. 4. The Coercivities decrease with the increase in crystallite size. Room temperature ferromagnetic behavior is exhibited by the $Zn_{1-x}Co_xO$ ($0.05 \leq x \leq 0.2$) samples.

4. CONCLUSIONS

XRD and detailed structural characterizations using X-ray absorption spectroscopy indicate that Co^{2+} substitute for Zn^{2+} in the tetrahedral configuration without forming secondary phases. The magnetic measurements indicate that two magnetic phases are present, with a ferromagnetic one dominating at high temperatures. Measurements at different compositions are in course in order to clarify the origin of this magnetic behaviour.

REFERENCES

1. H. Ohno, *Science* **281**, 951 (1998).
2. G.A. Prinz, *Science* **282**, 1660 (1998).
3. S. Maensiri, P. Laokul, S Phokha, *J. Magn. Magn. Mater.* **305**, 381 (2006).
4. K. Ueda, H. Tabata, T. Kawai, *Appl. Phys. Lett.* **79**, 988 (2001).
5. E. Bacaksiz, B. Maksu, M. Basol, M. Altunbaş, E. Yanmaz, *Thin Solid Films* **516**, 7899 (2008).
6. Q. Zeming, L. Aixia, S. Fenglian, S.Y. Liu, Z. Zhan, *Mater. Res. Bull.* **38**, 1791 (2003).
7. N. Murugesan, A. A. Suranaree, *Suranaree J. Sci. Technol.* **18** No 1, 81 (2011).
8. T. Fukumura, Z.W. Jin, A. Ohtomo, H. Koinuma, M. Kawasaki, *Appl. Phys. Lett.* **75**, 3366 (1999).

ACKNOWLEDGMENTS

The authors would like to thank the School of Engineering Sciences and Technology, Hyderabad University for providing EDS, FESEM, Sophisticated Analytical Instrument Facility, Northsern Eastern Hill University for TEM and special thanks to K. V. Rao, Head of Center of Nano Science and Technology, Jawaharlal Nehru Technological University Hyderabad.